

# Magnetic/NIR-thermally responsive hybrid nanogels for optical temperature sensing, tumor cell imaging and triggered drug release

Hui Wang, Jinhui Yi, Sumit Mukherjee, Probal Banerjee and Shuiqin Zhou\*

Department of Chemistry of The College of Staten Island and The Graduate Center, The City University of New York, Staten Island, NY 10314, USA

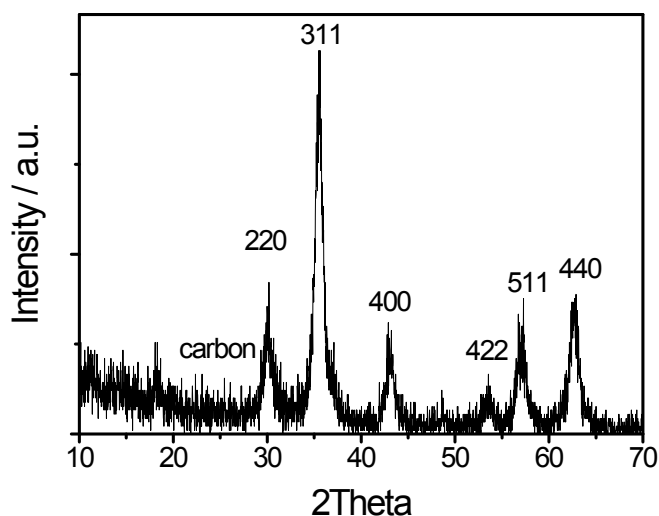


Figure S1. Typical XRD pattern of the as-obtained BFNPs.

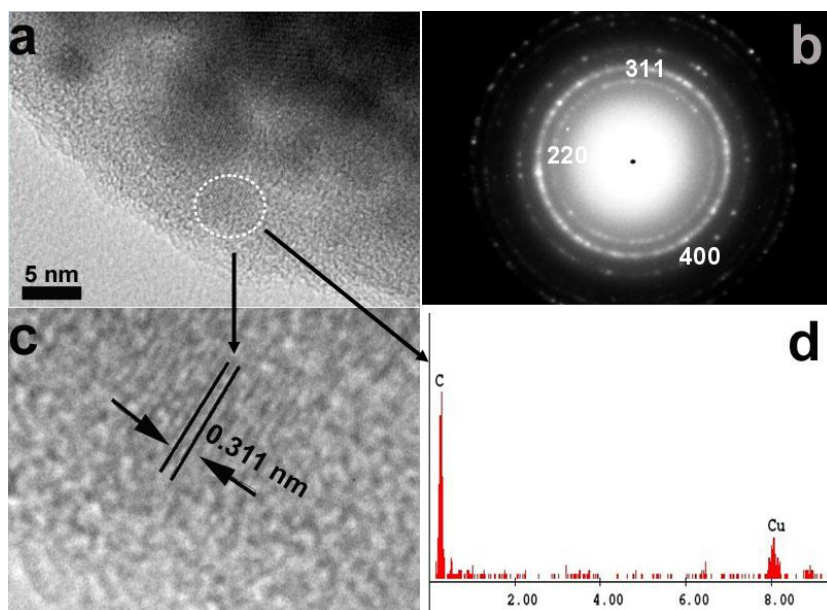


Figure S2. (a) High resolution TEM image and (b) electron diffraction (ED) pattern of the

BFNPs. (c) The lattice fringe and (d) Energy dispersive spectrum of carbon dot in the carbon shell, respectively.

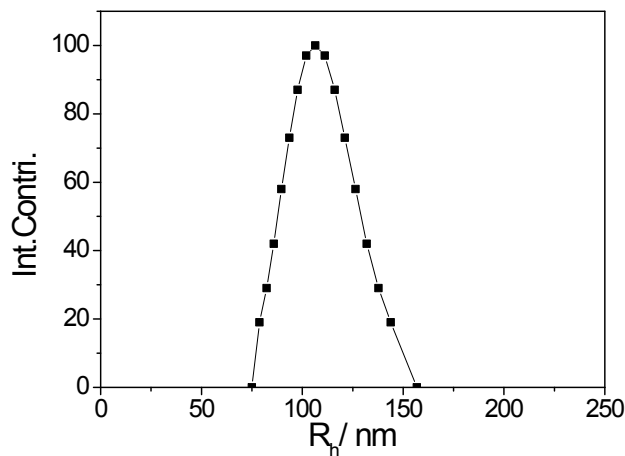


Figure S3. Hydrodynamic diameter distribution of BFNPs in PBS of pH = 7.40 measured at a scattering angle  $\theta=60^\circ$  and temperature of 24 °C.

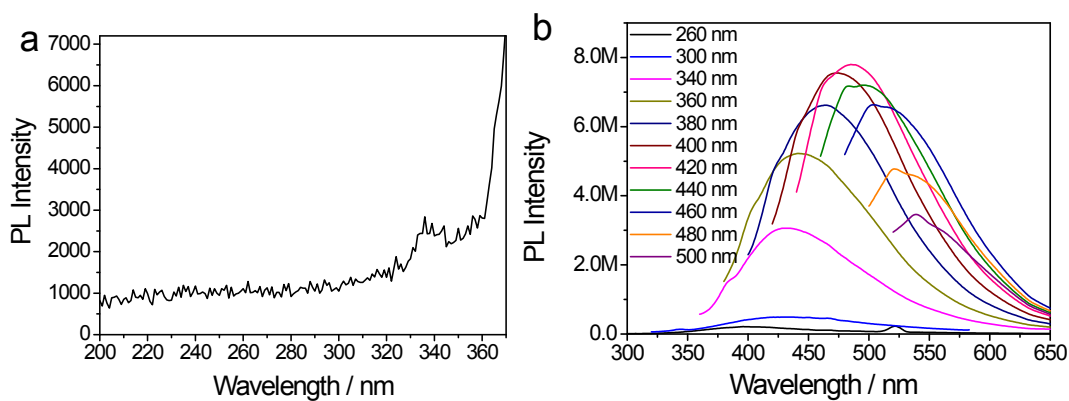


Figure S4. a) The excitation spectrum of the hybrid nanogels under a emission wavelength of 377 nm. (b) PL spectra of the hybrid nanogels under different excitation wavelengths.

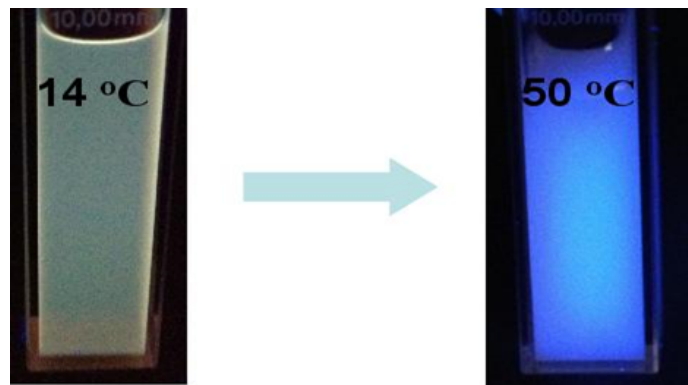


Figure S5. The photographs of the aqueous dispersions of poly(NIPAM-AAm)-BFNP hybrid nanogels at 14.0 °C and 50.0 °C, respectively, taken under 365 nm UV-lamp.

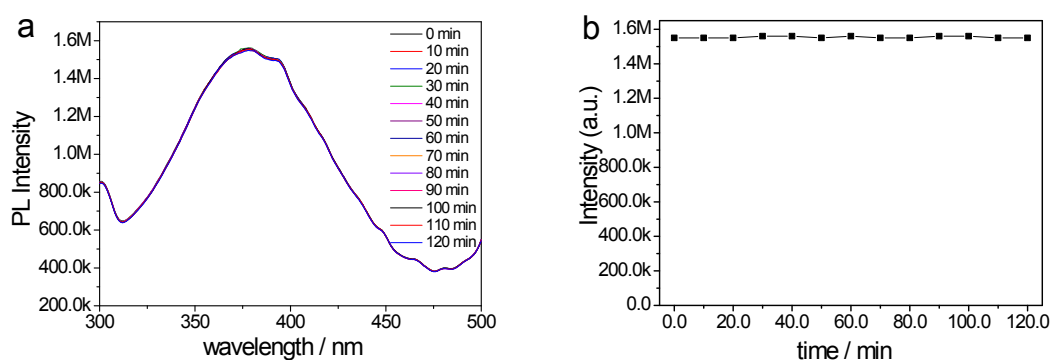


Figure S6. Fluorescence spectra ( $\lambda_{em}=377$  nm) (a) and intensity variation (b) of the hybrid nanogels under different excitation times from 0 min to 120 mins. Excitation wavelength = 264 nm.

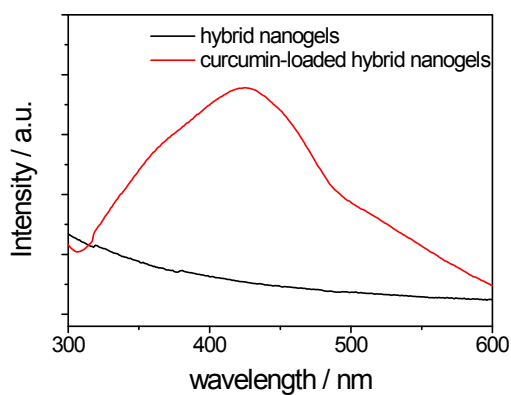


Figure S7. Typical UV-visible absorption spectra of the as-obtained hybrid nanogels and curcumin-loaded hybrid nanogels.



Figure S8. The photographs of aqueous solution of (left) curcumin and (right) curcumin-loaded hybrid nanogels.

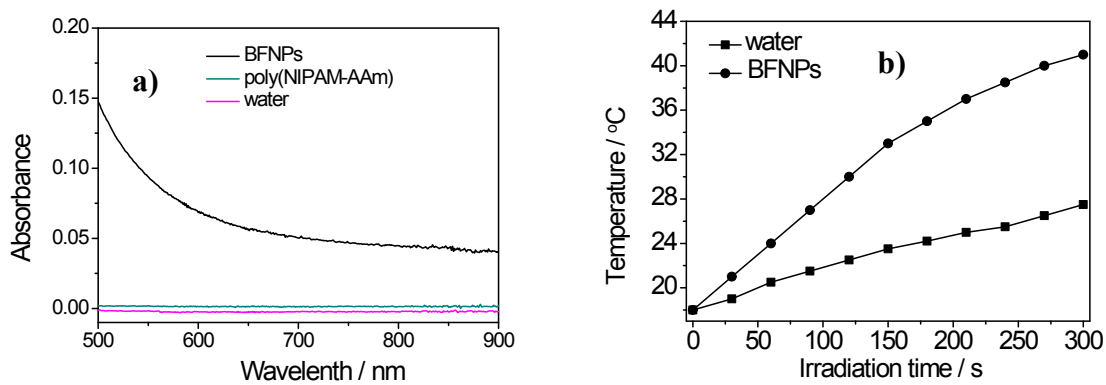


Figure S9. a) The Vis-NIR absorption spectrum of BFNPs (0.10 g/L in water), poly(NIPAM-AAm) nanogels, and water; b) The photothermal curves of BFNPs (0.10 g/L in water) and water under NIR irradiation for 5 min.

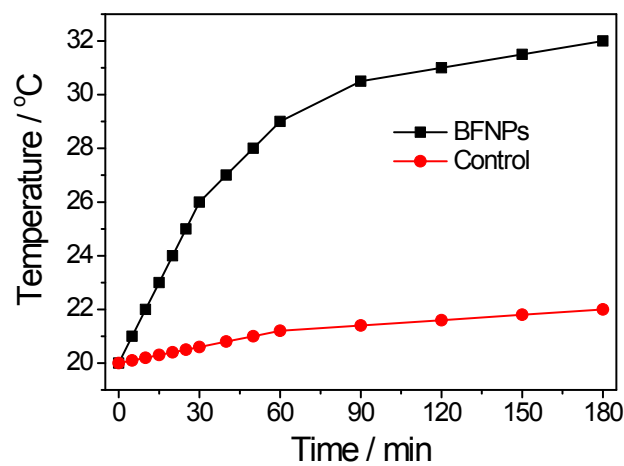


Figure S10. Hyperthermia assay on BFNPs (0.01 g/L in water) and water (control) under an alternating magnetic field.

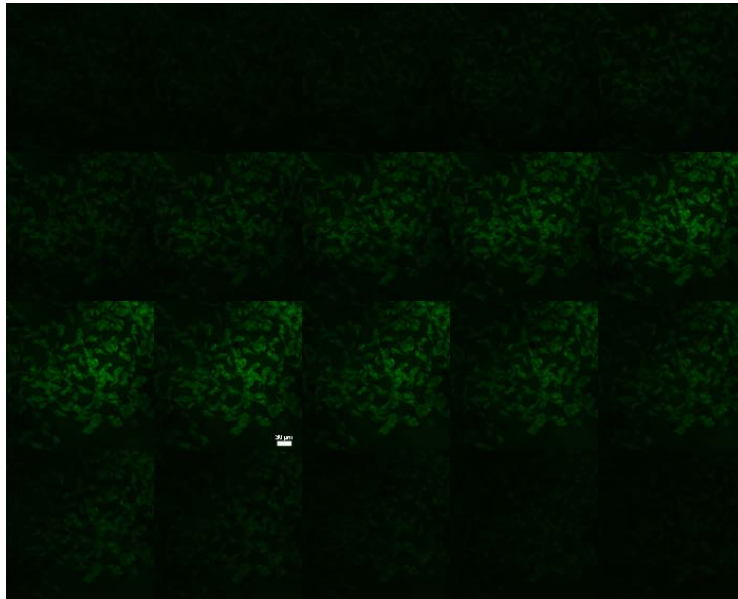


Figure S11. Z-Scanning confocal fluorescence images of the B16F10 cells incubated with the hybrid nanogels. Excitation wavelength = 405 nm.

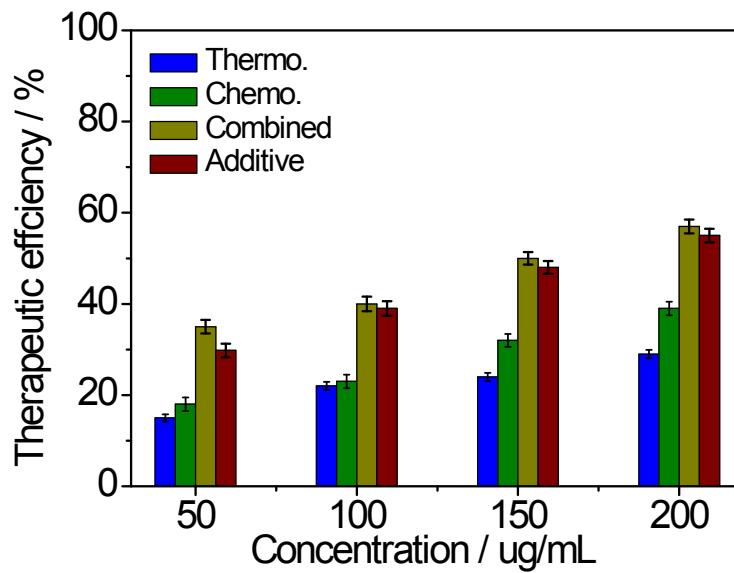


Figure S12. Comparison of the therapeutic efficacies of the hybrid nanogels as a drug carrier for NIR photothermal, chemo, and combined photothermal/chemo treatments.

Fig. S12 compares the therapeutic efficacies from the combined photothermal/chemo treatment (calculated by subtracting the cell viability from 100%) and the additive therapeutic efficacies ( $T_{\text{additive}}$ ) of chemo- and photothermal treatments. The  $T_{\text{additive}}$  was estimated using the relation of  $T_{\text{additive}} = 100 - (f_{\text{chemo}} \times f_{\text{photothermal}}) \times 100$ , where  $f$  is the fraction of surviving cells after each treatment.<sup>S1</sup> The therapeutic efficacy of combined photothermal/chemo treatments with the DOX-loaded hybrid nanogels was slightly higher than the additive therapeutic efficacy of chemo- and photothermal therapy alone.

#### Reference

S1 G. M. Hahn, J. Braun and I. Har-kedar, *Proc. Natl. Acad. Sci. U. S. A.*, 1975, **72**, 937.